THE JOURNAL OF BIOLOGICAL CHEMISTRY VOL. 284, NO. 42, pp. 28943–28952, October 16, 2009

Induced Dimerization of the Amyloid Precursor Protein Leads to Decreased Amyloid-β Protein Production*[S]

Received for publication, June 28, 2009, and in revised form, July 12, 2009 Published, JBC Papers in Press, July 13, 2009, DOI 10.1074/jbc.M109.038646

Simone Eggert, Brea Midthune, Barbara Cottrell, and Edward H. Koo[1]

From the Department of Neurosciences, University of California, San Diego, La Jolla, California 92093

The amyloid precursor protein (APP) plays a central role in Alzheimer disease (AD) pathogenesis because sequential cleavages by β- and γ-secretase lead to the generation of the amyloid-β (Aβ) peptide, a key constituent in the amyloid plaques present in brains of AD individuals. In several studies APP has recently been shown to form homodimers, and this event appears to influence Aβ generation. However, these studies have relied on APP mutations within the Aβ sequence itself that may affect APP processing by interfering with secretase cleavages independent of dimerization. Therefore, the impact of APP dimerization on Aβ production remains unclear. To address this question, we compared the approach of constitutive cysteine-induced APP dimerization with a regulatable dimerization system that does not require the introduction of mutations within the Aβ sequence. To this end we generated an APP chimeric molecule by fusing a domain of the FK506-binding protein (FKBP) to the C terminus of APP. The addition of the synthetic membrane-permeant drug AP20187 induces rapid dimerization of the APP-FKBP chimera. Using this system we were able to induce up to 70% APP dimers. Our results showed that controlled homodimerization of APP-FKBP leads to a 50% reduction in total Aβ levels in transfected N2a cells. Similar results were obtained with the direct precursor of β-secretase cleavage, C99/SPA4CT-FKBP. Furthermore, there was no modulation of different Aβ peptide species after APP dimerization in this system. Taken together, our results suggest that APP dimerization can directly affect γ-secretase processing and that dimerization is not required for Aβ production.

The mechanism of β-amyloid protein (Aβ)[2] generation from the amyloid precursor protein is of major interest in Alzheimer disease research because Aβ is the major constituent of senile plaques, one of the neuropathological hallmarks of Alzheimer disease (1, 2). In the amyloidogenic pathway Aβ is released from the amyloid precursor protein (APP) (3) after sequential cleavages by β-secretase BACE1 (4–6) and by the γ-secretase complex (7, 8). BACE1 cleavage releases the large ectodomain of APP while generating the membrane-anchored C-terminal APP fragment (CTF) of 99 amino acids (C99). Cleavage of β-CTF by γ-secretase leads to the secretion of Aβ peptides of various lengths and the release of the APP intracellular domain (AICD) into the cytosol (9–11). The γ-secretase complex consists of at least four proteins: presenilin, nicastrin, Aph-I, and Pen-2 (12). Presenilin is thought to be the catalytic subunit of the enzyme complex (13), but how the intramembrane scission is carried out remains to be elucidated. Alternatively, APP can first be cleaved in the non-amyloidogenic pathway by α-secretase within the Aβ domain between Lys-16 and Leu-17 (14, 15). This cleavage releases the APP ectodomain (APPsα) while generating the membrane-bound C-terminal fragment (α-CTF) of 83 amino acids (C83). The latter can be further processed by the γ-secretase complex, resulting in the secretion of the small 3-kDa fragment p3 and the release of AICD.

APP, a type I transmembrane protein (16) of unclear function, may act as a cell surface receptor (3). APP and its two homologues, APLP1 and APLP2, can dimerize in a homotypic or heterotypic manner and, in so doing, promote intercellular adhesion (17). *In vivo* interaction of APP, APLP1, and APLP2 was demonstrated by cross-linking studies from brain homogenates (18). To date at least four domains have been reported to promote APP dimerization; that is, the E1 domain containing the N-terminal growth factor-like domain and copper binding domain (17), the E2 domain containing the carbohydrate domain in the APP ectodomain (19), the APP juxtamembrane region (20), and the transmembrane domain (21, 22). In the latter domain the dimerization appears to be mediated by the G*XXX*G motif near the luminal face of the transmembrane region (21, 23). In addition to promoting cell adhesion, APP dimerization has been proposed to increase susceptibility to cell death (20, 24).

Interestingly, by introducing cysteine mutations into the APP juxtamembrane region, it was shown that stable dimers through formation of these disulfide linkages result in significantly enhanced Aβ production (25). This finding is consistent with the observation that stable Aβ dimers are found intracellularly in neurons and *in vivo* in brain (26). Taken together, these results have led to the idea that APP dimerization can positively regulate Aβ production. However, other laboratories have not been able to confirm some of these observations using slightly different approaches (23, 27).

* This work was supported, in whole or in part, by National Institutes of Health Grant AG 12376 (to E. H. K.). This work was also supported in part by a Deutsche Forschungsgemeinschaft postdoctoral fellowship (to S. E.).

[S] The on-line version of this article (available at http://www.jbc.org) contains supplemental Figs. 1–4.

[1] To whom correspondence should be addressed: Dept. of Neurosciences, University of California, San Diego, LBR, 9500 Gilman Drive, La Jolla, CA 92093. Tel.: 858-822-1024; Fax: 858-822-1021; E-mail: edkoo@ucsd.edu.

[2] The abbreviations used are: Aβ, amyloid-β peptide; APP, amyloid precursor protein; CTF, C-terminal (CT) fragment; MALDI-TOF, matrix-assisted laser desorption/ionization time of flight mass spectrometry; FKBP, FK506-binding protein; ELISA, enzyme-linked immunosorbent assay; DAPT, *N*-(*N*-(3,5-difluorophenylacetyl)-L-alanyl)-*S*-phenylglycine *t*-butyl ester; HA, hemagglutinin; AICD, APP intracellular domain; HA, hemagglutinin; wt, wild type; Bis-Tris, 2-[bis(2-hydroxyethyl)amino]-2-(hydroxymethyl)propane-1,3-diol; Tricine, *N*-[2-hydroxy-1,1-bis(hydroxymethyl)ethyl]glycine.

To further address the question of how dimerization of APP affects cleavage by α-, β-, and γ-secretase, we chose to test this with a controlled dimerization system. Accordingly, we engineered a chimeric APP molecule by fusing a portion of the FK506-binding protein (FKBP) to the C terminus of APP such that the addition of the synthetic membrane-permeant bifunctional compound, AP20187, will induce dimerization of the APP-FKBP chimera in a controlled manner by binding to the FKBP domains. Using this system, efficient dimerization of APP up to 70% can be achieved in a time and concentration-dependent fashion. Our studies showed that controlled homodimerization of APP-FKBP leads to decreased total Aβ levels in transfected N2a cells. Homodimerization of the β-CTF/C99 fragment, the direct precursor of γ-secretase cleavage, showed comparable results. In addition, induced dimerization of APP did not lead to a modulation of different Aβ peptides as it was reported for G*XXX*G mutants within the transmembrane domain of APP (21).

EXPERIMENTAL PROCEDURES

DNA Constructs—FKBP-tagged APP695 constructs were generated in a three-fragment ligation step. First, the 1054-bp EcoRI and XhoI 5′ fragment was released from APP695 pUAST (17). Second, an APP fragment from the 3′ end was generated by PCR from APP695 pUAST without a stop codon and appending an XbaI restriction site using the primer 5′-CGAGTTCCTACAACAGCAGCC-3′ and an antisense primer, 5′-GCGGTGTCTAGAGTTCTGCATCTGCTC-3′, and digested with XhoI and XbaI. These two fragments were ligated into the vector pC4F1 (with one FKBP domain) or pC4F2 (with two FKBP domains) (Ariad Pharmaceuticals, Cambridge, MA) using the restriction sites EcoRI and XbaI. To generate FKBP-tagged SPA4CT constructs, a silent mutation was first introduced into SPA4CT DA pCEP4 (28) at position Glu-22 (Aβ numbering) to remove the internal EcoRI site by site-directed mutagenesis (QuikChange, Stratagene, La Jolla, CA). A PCR fragment of the entire SPA4CT DA open reading frame was subsequently generated, again without the stop codon and with an Xba1 site added to the 3′ end and an EcoRI site added to the 5′end, and ligated into vector pC4F1 (with one FKBP domain) and vector pC4F2 (with two FKBP domains). A control FKBP-tagged AICD construct starting at Val-50 (Aβ numbering) was generated with a methionine residue added as a start codon and ligated into pC4F1 (or pC4F2).

To generate an APP695 CT HA construct without the FKBP fusion, the 3′-untranslated region of APP was amplified from APP695 wt NT HA pcDNA3.1 neo (17) with sense primer 5′-GTTTATAACTCGAGACCCCCGCCACAGC-3′, containing an XhoI site, and antisense primer, 5′-CCCGCGGCTCTAGATCTTAAAGCATATGTAAAG-3′, containing an XbaI site. The PCR product was digested with XhoI and XbaI restriction enzymes and subcloned into the same sites in the pcDNA3.1+ neo vector. Sense primer 5′-GTGGCCGAGGAGGAGATTCAGGA-3′, starting at position 1481 in the APP695 open reading frame and antisense primer, 5′-GCTGACCTCGAGTTATGCGTAGTCTGGTACGTCGTACGGATAGTTCTGCATCTGCTC-3′, containing the 3′ end of the APP695 open reading frame without a stop codon, the HA tag, and an XhoI restriction site, were used to amplify APP695 wt NT HA. The PCR product was digested with SacI and XhoI restriction enzymes. The EcoRI and SacI fragment from APP695 pUAST and the preceding SacI-XhoI 1736-bp PCR fragment were ligated into the EcoR1 and XhoI sites in the pcDNA3.1+ neo vector containing the 3′-untranslated region of APP. Subsequently, the L17C, K28C, K28S, and K28A mutations were introduced into the APP695 CT HA pcDNA3.1+ neo plasmid by site-directed mutagenesis (QuikChange).

Antibodies, Cell Lines, Transfections, and Cell Culture—Mouse Neuroblastoma N2a cells were maintained in Dulbecco's modified Eagle's medium supplemented with 10% fetal bovine serum and 1% penicillin/streptomycin. N2a cells were plated in 6-well plates and transfected with Lipofectamine 2000 according to the manufacturer's instructions. The dimerizing ligand, AP20187 (Ariad Pharmaceuticals), was added 7 h after transfection and continued from 1 to 17 h. Monoclonal antibodies included HA.11 to detect the HA epitope tag (Covance), 82E1 against the free N terminus of Aβ (IBL, Minneapolis MN), B436 recognizing the N-terminal region of Aβ (29), and 6E10 (Signet), WO2 (30), and Ab9 (31) against the amino acids 1–16 of human Aβ. The polyclonal sAPPβ antibody recognizes the ISEVKM sequence at the C terminus of wild type human sAPPβ (Immuno-Biological Laboratories, Inc., Minneapolis, MN). Antibody 6E10 was also used for detection of sAPPα, and β-secretase cleavage site-specific antibody 82E1 was also used for detection of the APPβ C-terminal fragment. The β-tubulin antibody E7-a1 was obtained from Developmental Studies Hybridoma Bank.

SDS Electrophoresis and Immunoblotting—Cells were lysed for 15 min at 4 °C in lysis buffer (50 mM Tris/HCl, pH 7.5, 150 mM NaCl, 5 mM EDTA, and 1% Nonidet P40) supplemented with protease inhibitors (Complete™ protease inhibitor mixture, Roche Applied Science). The supernatants were collected, and the protein concentration determined with a Micro BCA assay (Pierce). Equal amounts of protein samples were separated on 8 or 12% Bis-Tris SDS-PAGE or 12.5 or 15% Tris/glycine SDS-PAGE and then transferred to nitrocellulose membranes. To separate Aβ38, Aβ39, Aβ40, and Aβ42 species, media samples were immunoprecipitated with antibody B436 as above and separated on 10% Tris/Tricine gels containing 8 M urea (32). Synthetic Aβ peptide standards (AnaSpec) were separated in parallel with the experimental samples. After electrophoresis and transfer to nitrocellulose, the membranes were incubated with 82E1 monoclonal antibody which recognizes all full-length Aβ peptides starting at position 1.

Blue Native Gel Electrophoresis—Blue native gel electrophoresis was performed according to a protocol modified from Schägger *et al.* (33). In brief, cells in one 10-cm cell culture dish were washed once and collected in phosphate-buffered saline at 4 °C. The cell pellets were resuspended in 1 ml of homogenization buffer (250 mM sucrose in 20 mM HEPES, pH 7.4, with protease inhibitors) and then sheared by passing through a 27 × gauge needle 10 times. Postnuclear supernatant was collected after a low speed spin at 1000 × *g* for 15 min at 4 °C. The membranes were pelleted after centrifugation at 100,000 × *g*

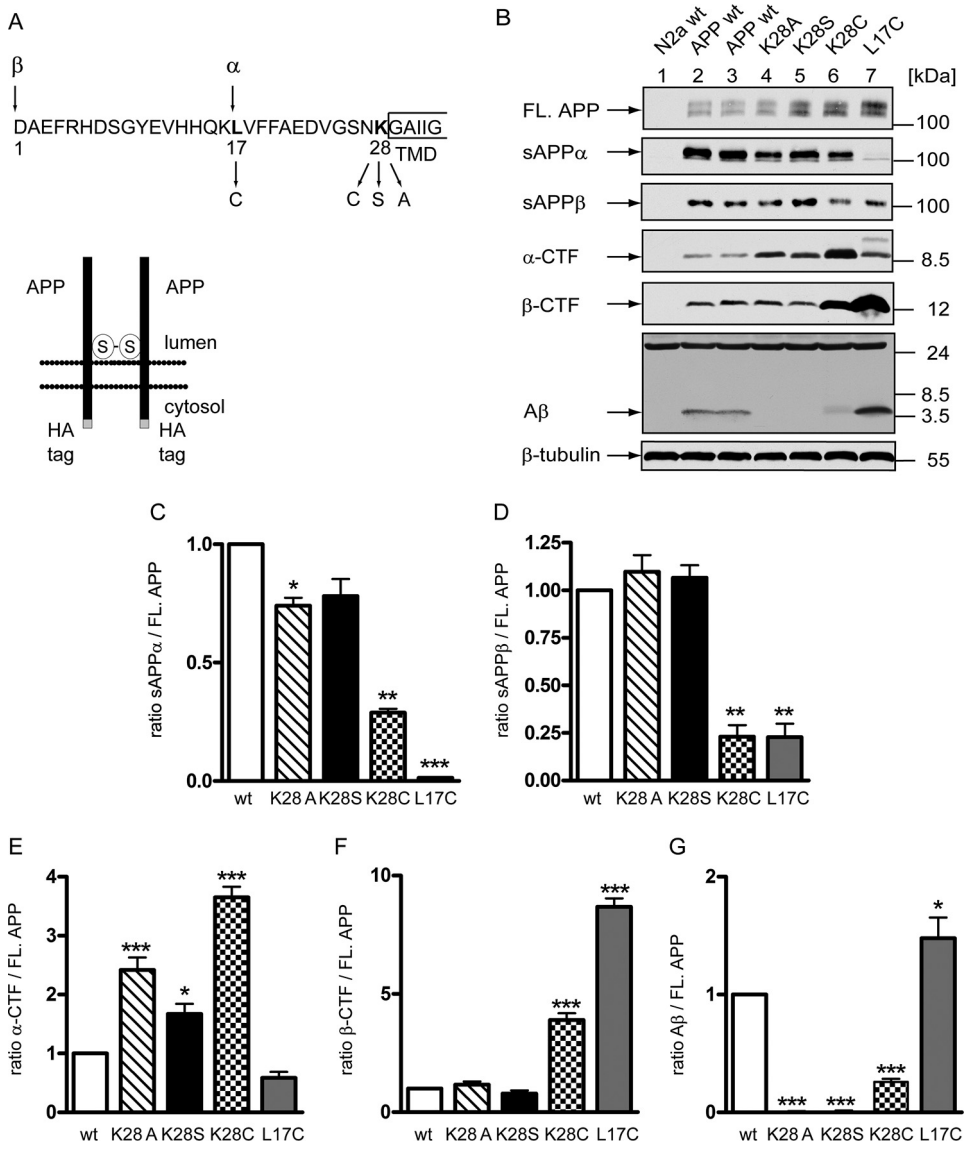

FIGURE 1. **Contrasting effects on Aβ levels with L17C and mutations at K28.** *A*, schematic representation of the position of the APP mutants used and of the cysteine disulfide-bridge-induced dimerization (21, 25) of APP. *B*, N2a cells were transiently transfected with the construct APP695 CT HA and the four respective mutants: L17C, K28C, K28S, K28A. Cell lysates were analyzed via Western blotting of full-length (*FL*) APP and various different APP cleavage products. Full-length APP and α-CTFs were immunoblotted with an HA antibody, β-CTFs were detected with β-cleavage site-specific antibody 82E1. Detection of the same protein samples with a β-tubulin antibody served as a loading control. Conditioned media were immunoprecipitated with Aβ antibody B436 followed by Western blotting with Aβ antibody 82E1. Immunoblotting of sAPPα and sAPPβ in the media were detected by 6E10 and sAPPβ specific antibodies, respectively. Quantification of blots shown in *panel B*: *C*, sAPPα; *D*, sAPPβ; *E*, α-CTF; *F*, β-CTF; *G*, Aβ. Results are from an average of three independent experiments ±S.D. normalized to the APP wt control, one-way analysis of variance followed by Tukey's post hoc analyses (*, $p < 0.05$; **, $p < 0.01$; ***, $p < 0.001$).

for 1 h at 4 °C and washed once with 200 μl of homogenization buffer, and the centrifugation was repeated once. The pellets containing the membranes were resuspended in 200 μl of homogenization buffer. 100 μg of protein were solubilized with Blue Native sample buffer (1.5 M amino caproic acid, 0.05 M Bis-Tris, 10% *n*-dodedecyl-β-D-maltoside, and protease inhibitor at pH 7.5). The samples were incubated on ice for 30 min and then centrifuged for 10 min at 14,000 rpm at 4 °C in a microcentrifuge. Blue Native loading buffer (5.0% Serva Coomassie Brilliant Blue G250 and 1.0 M aminocaproic acid) was added to the supernatant. The samples were separated on 4–15% Tris-HCl gels (Criterion, Bio-Rad) overnight at 4 °C with Coomassie Blue containing cathode buffer (10× cathode buffer, pH 7.0, 0.5 M Tricine, 0.15 M Bis-Tris, 0.2% Coomassie Blue) and anode buffer (pH 7.0, 0.5 M Bis-Tris). The gel was transferred to a polyvinylidene difluoride membrane. The following molecular weight standards were used: thyroglobulin (669 kDa), apoferritin (443 kDa), catalase (240 kDa), aldolase (158 kDa), and bovine serum albumin (66 kDa), all from Sigma.

Immunoprecipitation of Aβ—N2a cells in six-well plates were transiently transfected with Lipofectamine 2000 according to the manufacturer's instructions. Overnight conditioned media were collected and incubated overnight at 4 °C with antibody B436 and anti-mouse IgG-agarose beads (American Qualex, San Clemente, CA). After 3 washes with buffer A (10 mM Tris-HCl, pH 7.5, 150 mM NaCl, 2 mM EDTA, 0.2% Nonidet P-40) and 1 wash with 10 mM Tris-HCl, pH 7.5, the beads were resuspended in 2× Laemmli sample buffer plus dithiothreitol and separated by 12% Bis-Tris SDS-PAGE.

ELISA—Aβ40 and Aβ42 species were quantified with sandwich ELISAs essentially as described (34). In brief, 100 μl of diluted media were analyzed on Immulon 4 HBX plates (Thermo Scientific, Waltham, MA) that were coated before with 25 μg/ml concentrations of the capture antibody in phosphate-buffered saline. For Aβ40, Ab9 was the capture antibody, and horseradish peroxidase-conjugated 13.1.1 (epitope Aβ-(35–40)) was the reporter antibody. For Aβ42, antibody 2.1.3 (epitope, Aβ-(35–42)) was the capture antibody, whereas horseradish peroxidase-conjugated Ab9 was the reporter antibody. The signal was developed with TMB (3,3′,5,5′-tetramethylbenzidine) solution and measured in an ELISA plate reader. All measurements were performed in triplicate.

Mass Spectrometry Analysis—Matrix-assisted laser desorption/ionization time of flight (MALDI-TOF) mass spectrometry of Aβ peptides was performed on a 4800 MALDI-TOF-TOF (Applied Biosystems/MDS-Sciex, Foster City, CA). Aβ peptides were immunoprecipitated from conditioned medium with antibody B436 coupled to Seize™ beads (Pierce). The

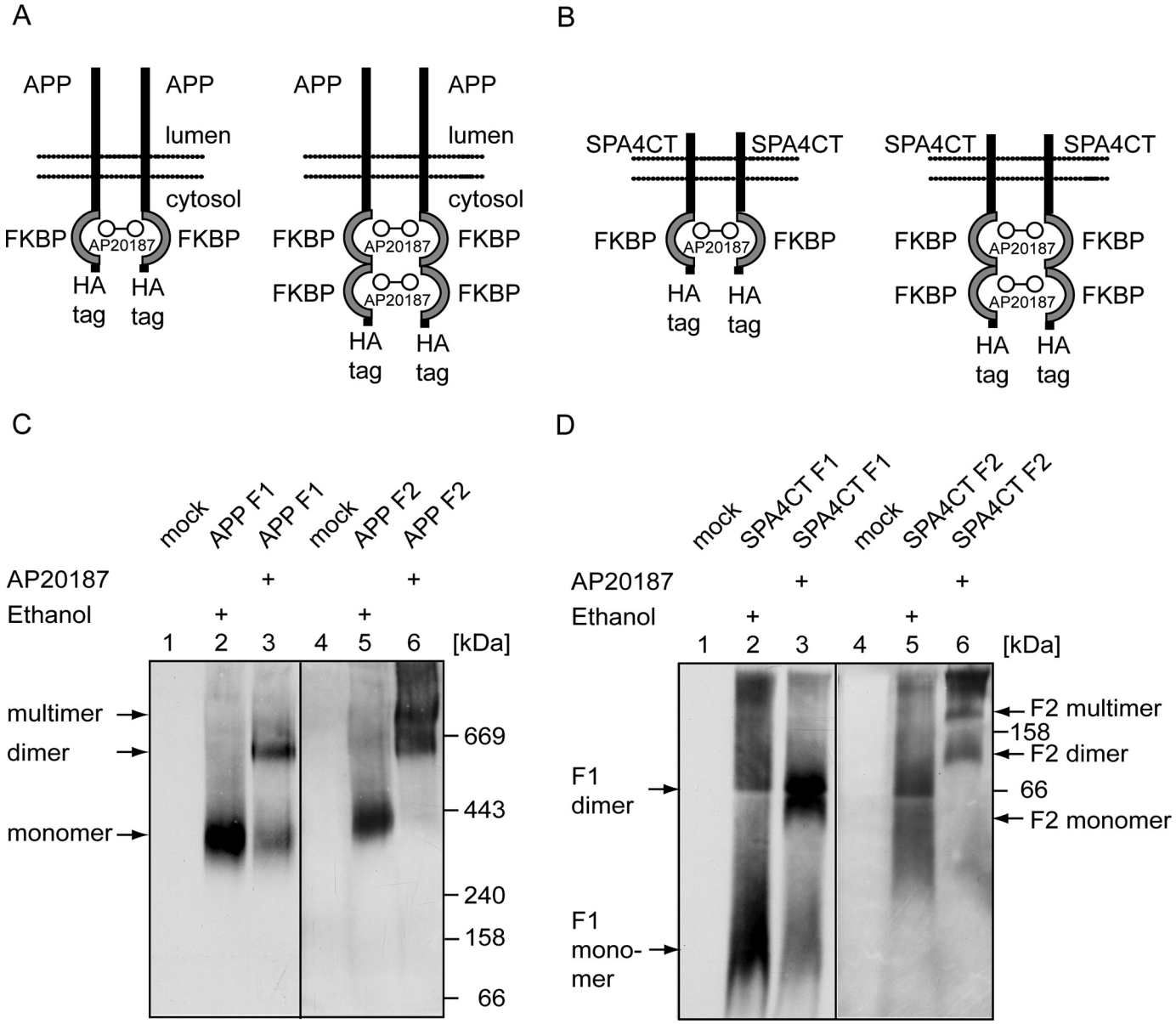

FIGURE 2. **Induced dimerization of C-terminal FKBP-tagged APP695 and SPA4CT analyzed by Blue Native gel electrophoresis.** *A*, schematic representation of APP695 F1 and APP695 F2 constructs consisting of an APP695-FKBP fusion protein with a C-terminal HA tag. APP695 F1 contains one 12-kDa FKBP tag, and APP695 F2 contains two FKBP tags fused in a tandem repeat. AP20187 is an analogue of rapamycin, which binds to FKBP, thereby inducing dimerization of APP-FKBP fusion proteins. *B*, schematic representation of the constructs SPA4CT F1 and SPA4CT F2, containing one FKBP or two FKBP tags, respectively. *C* and *D*, dimerization was induced with AP20187 (100 nM) overnight in N2a cells transiently transfected with APP695 F1/APP695 F2 (*C*) or with SPA4CT F1/SPA4CT F2 (*D*). Note, formation of dimers and multimers in the APP chimeric proteins seen by Blue Native PAGE followed by Western blotting with anti-HA antibody.

immunoprecipitates were eluted from the beads with 25% 0.1% trifluoroacetic acid, 75% acetonitrile, and the resulting samples were mixed 1:1 with α-cyano-4-hydroxycinnamic acid matrix in methanol:acetonitrile:water (36:56:8) (Agilent, Santa Clara, CA) and spotted on the MALDI target grid. Mass spectra were acquired from m/z 3,500–5,000 Da in reflector positive mode at 10,000 shots/spectrum using single shot protection and delayed extraction times of 420 ns. The mass spectra are plotted as m/z *versus* relative intensity.

RESULTS

Cysteine Induced Dimerization of APP—Studies from Multhaup and co-workers (25) have shown that artificial dimerization of APP by introducing cysteine residues within the Aβ domain increased Aβ production. K28C mutation (using Aβ numbering) showed 6–7-fold augmentation in Aβ secretion (25), whereas the L17C mutation (21) showed unchanged Aβ40 levels but increased Aβ42 release, suggesting that dimers of APP facilitate Aβ generation. However, a recent study reported that a K28S mutation showed a marked (90%) reduction in Aβ production (35), possibly due to impairment in γ-secretase cleavage. As a result, we wish to first revisit these cysteine mutants as well as determine the effects of base substitutions at the lysine residue at position 28 (by Aβ numbering or position 624 by APP695 numbering). Accordingly, we examined APP

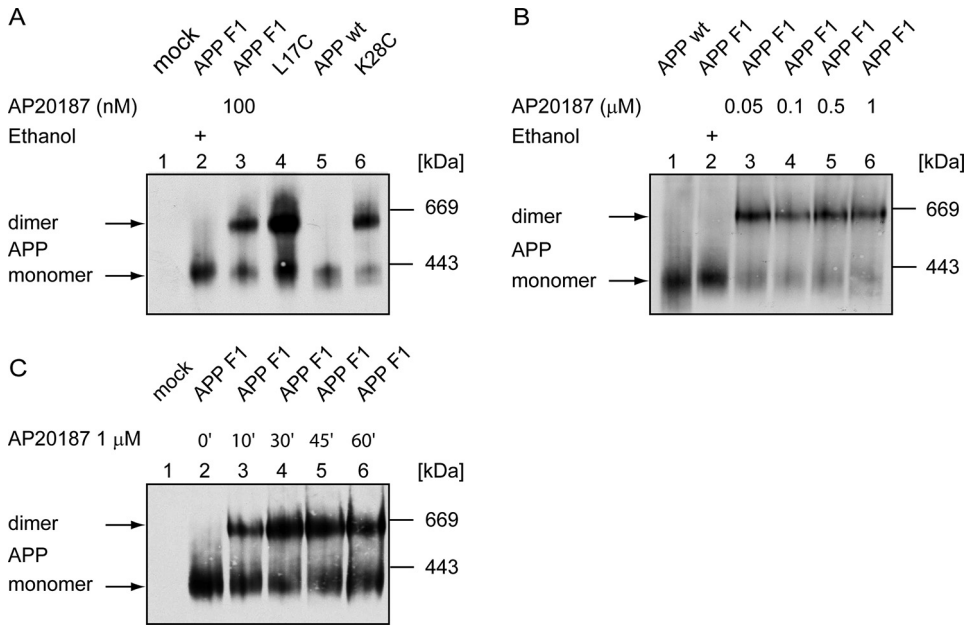

FIGURE 3. **APP dimers in various APP constructs analyzed by Blue Native gel electrophoresis.** *A*, N2a cells were transiently transfected with APP695 F1, APP695 CT HA wt, APP695 CT HA L17C, and APP695 CT HA K28C. Dimerization of APP695 F1 was induced with 100 nM AP20187 overnight, and controls were ethanol-treated cells as well as APP cysteine mutants. *B*, N2a cells were transiently transfected with the APP695 F1 construct and then treated overnight with various concentrations of AP20187 (0.05, 0.1, 0.5, and 1 μM). *C*, time course of induced dimerization of APP. APP dimerization was induced in N2a cells transiently transfected with APP695 F1 after treatment with 1 μM AP20187 from 0 to 60 min. In *A–C*, samples were analyzed via Blue Native PAGE followed by Western blotting with an anti-HA antibody.

processing and Aβ production in four different mutations: L17C, K28C, K28S, and K28A (Fig. 1*A*). All three mutations at Aβ28 (K28A, K28C, and K28S) resulted in a significant reduction in Aβ secretion. For K28A and K28S, the Aβ levels were essentially undetectable. The magnitude of reduction in Aβ production in the K28C mutation was slightly variable, depending on the Aβ antibody used for immunoprecipitations (supplemental Fig. 1). In parallel, there was a strong reduction in sAPPα secretion in the L17C mutant, indicating that impairment of α-secretase cleavage might have led to increased β-secretase cleavage, as seen in the concomitant rise in the level of β-CTF. Although there was a mild reduction in sAPPα and sAPPβ secretion in the K28C mutant, neither the K28A nor the K28S mutant showed any significant alterations in sAPPβ secretion. In addition, there was a substantial change in α-secretase processing for mutants K28S and K28A. Nevertheless, our findings are consistent with those reported by Ren *et al.* (35) that substitutions of the basic lysine residue at position 28 by other hydrophilic (Cys or Ser) or hydrophobic (Ala) amino acids led to marked reduction in Aβ production, presumably by affecting γ-secretase cleavage. However, in view of the K28C results it appears that dimerized APP does not consistently augment Aβ generation, especially if the K28C substitution led to other perturbations in APP processing.

Blue Native Gel Analysis of Induced and Constitutive Dimerization of APP695 and C99—In light of the above results, another approach to dimerize APP is needed to determine the impact of APP dimerization on Aβ production, especially one that minimizes secondary effects due to amino acid substitutions within the Aβ sequence. We used a regulated homodimerization system based on the human FKBP12 and a small bifunctional ligand, AP20187 (36). We engineered a chimeric APP construct containing the full-length human APP cDNA fused to one or two FKBP domains and a HA epitope tag at the C terminus (Fig. 2*A*). AP20187, an analogue of rapamycin, is a membrane-permeable compound that induces rapid dimerization of the FKBP or, in this case, APP695-FKBP. Either one FKBP domain (APP F1) or two FKBP domains (APP F2) were fused to the C terminus of APP to enable APP dimerization. To analyze the impact of APP dimerization on γ-secretase processing directly, we also fused one or two FKBP domains to a C99 or β-CTF construct, SPA4CT, as above, and these are termed SPA4CT F1 and F2, respectively (Fig. 2*B*). SPA4CT mimics the C99 β C-terminal fragment generated after BACE1 cleavage and is a direct substrate of γ-secretase cleavage (28).

To examine dimerization of these APP-FKBP chimeric constructs, APP695 F1 and APP695 F2 were transiently transfected into mouse N2a cells and treated overnight with AP20187. Blue Native PAGE showed that the majority of APP molecules were in the dimer form (about 70%), whereas the untreated control sample showed very little APP dimers (Fig. 2*C*). For comparison, both APP cysteine mutants (APP L17C and K28C) showed comparable levels of APP dimer formation using Blue Native PAGE (Fig. 3*A*). Dimerization of APP F2 was more efficient than APP F1 due to the additional FKBP domain with almost no APP monomer present (Fig. 2*C*). In addition, APP multimers, likely tetramers, were also detected. Of note, in the Blue Native gel system, the APP monomer migrated with a mobility of ~300 kDa (Fig. 2*C*), whereas the APP dimer had a molecular mass of twice the monomer size (~600 kDa). The apparent molecular mass of APP monomers and dimers in this gel system is in accordance with a recent publication by Sato *et al.* (37) and likely does not reflect their true molecular masses. This is consistent with the observation that migration of the two APP cysteine mutants was essentially the same as the APP-FKBP chimeric proteins using Blue Native PAGE (Fig. 3*A*). Furthermore, in non-reducing and SDS-denaturing gels, the cysteine mutants migrated at the predicted molecular masses and showed comparable ratios of monomers and dimers as seen in the Blue Native gels (supplemental Fig. 1).

In the SPA4CT F1 construct the addition of AP20187 also led to about 70% dimerization, similar to what was observed for APP F1 (Fig. 2*D*). Similarly, dimerization of SPA4CT F2 showed strong formation of dimers and higher order mul-

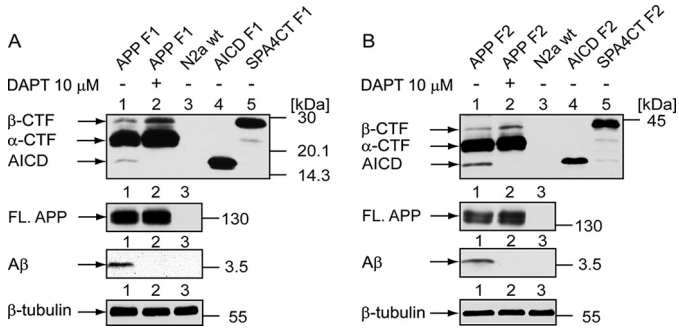

FIGURE 4. **APP695 F1 and APP695 F2 constructs are processed normally by γ-secretase.** N2a cells were transiently transfected with APP695 F1 (*A*) or APP695 F2 (*B*) and treated with 10 μM concentrations of the γ-secretase inhibitor DAPT for 8 h (*lane 2*). AICD, which co-migrated with a control AICD F1 (or AICD F2) construct, can be detected from both APP full-length (*FL*) constructs, and generation of this fragment can be blocked by DAPT. Similarly, Aβ is released into the medium in a DAPT-dependent manner from both APP F1 and APP F2 constructs. Full-length APP and CTFs in the cell lysates were immunoblotted with an anti-HA antibody, and β-tubulin was detected with antibody E7. Aβ was immunoprecipitated from conditioned medium with Aβ antibody B436 and immunoblotted with β-site-specific 82E1 antibody.

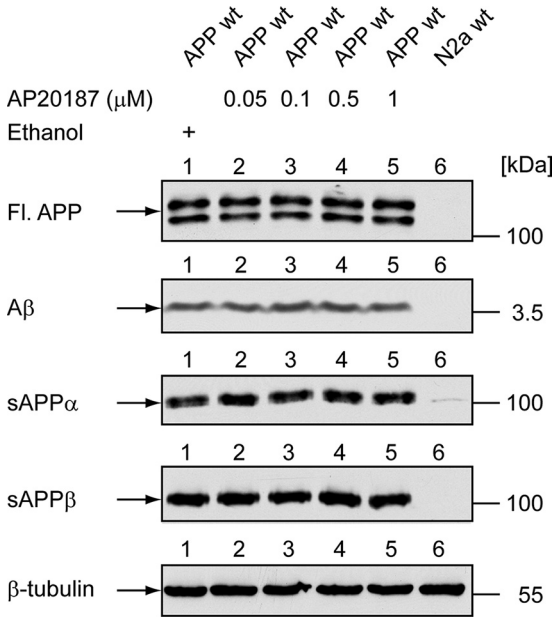

FIGURE 5. **AP20187 does not affect APP695 wt processing.** N2a cells stably expressing wild type full-length (*FL*) APP695 (without FKBP tag) were treated with increasing concentrations of AP20187 overnight. Cell lysates were analyzed via immunoblotting with antibody 6E10 for APP and antibody E7 for β-tubulin. Aβ was immunoprecipitated with antibody B436 and immunoblotted with antibody 82E1. sAPPα and sAPPβ in the media were detected by immunoblotting with 6E10 and sAPPβ-specific antibodies, respectively.

timers with almost complete absence of the monomeric species (Fig. 2*D*).

To determine the dose response of APP-FKBP chimeric protein to AP20187, APP F1-transfected cells were incubated overnight with different concentrations of AP20187 (50 nM, 100 nM, 500 nM, and 1 μM). After Blue Native gel electrophoresis, essentially the same level of dimerization (~70%) was seen in all four concentrations of AP20187 after overnight treatment (Fig. 3*B*). To determine the time course of dimerization, APP F1-transfected cells were incubated with either 500 nM or 1 μM AP20187 and analyzed from 10 to 60 min after treatment. Both concentrations led to rapid dimerization such that abundant dimers were present after only 10 min of treatment in accordance with previously published studies using this system (Fig. 3*C* for 1 μM, data not shown for 500 nM). Therefore, dimerization of the APP-FKBP chimera with AP20187 was rapid and efficient. The level of induced dimerization was also comparable with the APP cysteine mutants but has the advantage of not altering any Aβ amino acid residues.

APP695 F1 and APP695 F2 Are Functional γ-Secretase Substrates—To confirm that the addition of the FKBP sequences to the C terminus of APP did not perturb Aβ generation, APP695 F1 and APP695 F2 were transiently transfected into N2a cells, and the cells were analyzed for APP processing (Fig. 4). Abundant APP CTFs and AICD were detected in cells transfected with either construct. The latter species were confirmed by mobility to AICD F1 or AICD F2 control constructs, and production of this fragment was abolished after treatment with the γ-secretase inhibitor DAPT. The stability of AICD is likely due to the presence of the FKBP tag because a number of reports have shown stabilization of AICD after fusion with various protein tags (9, 38–40). Furthermore, high levels of Aβ were released from cells transfected with the APP F1 and APP F2 constructs, indicating no overt perturbation of γ-secretase cleavage. DAPT treatment inhibited Aβ production as well as AICD production from cells transfected with APP F1 and APP F2 (Fig. 4).

Dimerization of APP695 F1 Leads to Decreased Aβ Production—We next assessed the effects of induced dimerization on APP proteolytic processing. However, we first wish to ascertain that AP20187 does not by itself alter APP processing or Aβ generation. Accordingly, N2a cells stably transfected with wild type full-length APP695 (without the FKBP tag) were treated with increasing doses of AP20187. Indeed, at concentrations up to 1 μM, we did not detect any appreciable changes in full-length APP or in the levels of secreted sAPPα, sAPPβ, Aβ, indicating that this compound does not perturb APP metabolism (Fig. 5). Next, N2a cells were transiently transfected with the APP F1 construct and then treated overnight with 50 or 100 nM AP20187. After this treatment, steady state levels of full-length APP were consistently higher than control cells not treated with AP20187 (Fig. 6*A*). Levels of Aβ were essentially unchanged, but when corrected for the increased APP levels, there was a significant 50% reduction in Aβ secretion. Interestingly, AICD and β-CTF levels were slightly increased, whereas α-CTFs, sAPPα, and sAPPβ levels showed a mild reduction or no change. Similar results were obtained with the APP F2 construct (supplemental Fig. 2). In addition, similar changes were seen in intracellular Aβ levels after AP20187 treatment, suggesting that APP-FKBP-induced dimerization did not result in a selective retention of Aβ in intracellular compartments (supplemental Fig. 4).

Because it has been suggested that dimerization of APP modulates the production of shorter Aβ species (21), we proceeded to determine whether dimerization of APP695 induced by AP20187 resulted in the generation of different Aβ species. Therefore, media of N2a cells transfected with the APP695 F1 construct and treated with 50 and 100 nM AP20187 were analyzed on Tricine-urea gels to separate the

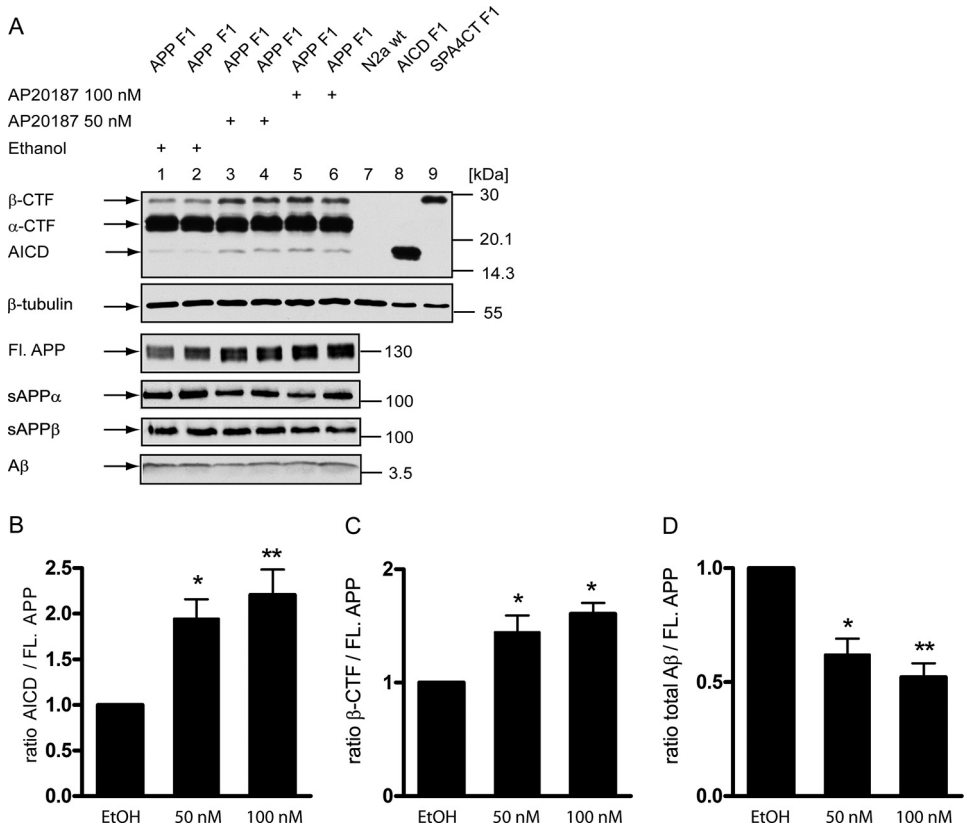

FIGURE 6. **Processing of APP695 F1 after induced dimerization.** N2a cells were transiently transfected with APP695 F1, and dimerization was induced with 50 and 100 nM AP20187 overnight. *A*, cell lysates from N2a cells transiently transfected with APP695 F1 and treated overnight with AP20187 (50 or 100 nM) were analyzed by immunoblotting for full-length (*FL*) APP, CTFs, and AICD with anti-HA antibody. Conditioned media were immunoblotted by antibody 6E10 for sAPPα and an sAPPβ-specific antibody for sAPPβ. Immunoprecipitation of total Aβ in the media was carried with Aβ antibody B436 and immunoblotting followed with antibody 82E1. Quantification of AICD (*B*), β-CTF (*C*), and Aβ (*D*) from blots from three independent experiments is shown in *panel A* ±S.D. (one-way analysis of variance followed by Tukey's post hoc analyses. *, $p < 0.05$; **, $p < 0.01$; ***, $p < 0.001$).

various Aβ species (Fig. 7*A*). By this approach the profile of Aβ-(38–42) peptides from the APP695 F1 construct (and the APP695 F2 construct, data not shown) was essentially unchanged, with Aβ40 being the predominant species as expected. Quantification of the different Aβ species from three independent experiments showed no significant change in their ratios. Finally, Aβ from cells transiently transfected with APP F1 or APP F2 were analyzed by MALDI-TOF after treatment with 500 nM AP20187 (Fig. 7, *B* and *C*). The results showed that there were no substantial changes in Aβ species from either APP F1 or APP F2 cells with or without AP20187 treatment. Taken together, our results showed that induced dimerization of APP reduced Aβ levels without modulation of individual Aβ species.

Dimerization of C99 Leads to Decreased Aβ Production—The above results suggested that dimerization of APP lowers Aβ generation, possibly at the level of γ-secretase cleavage. To confirm this interpretation, we next analyzed the processing of SPA4CT, the β-CTF fragment generated after BACE1 cleavage. Accordingly, we assessed Aβ and AICD levels in cells transfected with the C99/SPA4CT F1 or C99/SPA4CT F2 constructs, both of which can be efficiently dimerized (see Fig. 2*D*). Treatment with AP20187 led to an increase in C99/β-CTF fragment and AICD levels (Fig. 8*A*, supplemental Fig. 3), similar to the observations with full-length APP (see Fig. 6, supplemental Fig. 2). When normalized to steady state levels of β-CTF, levels of secreted total Aβ were markedly diminished (70–80%) in cells treated with 100 nM AP20187. The medium was also analyzed by ELISA to quantify the relative levels of Aβ40 and Aβ42 production (Fig. 8, *D* and *E*). Indeed, both species were reduced by ~70%, with slightly more reduction seen for the Aβ40 peptides. In sum, studies with both full-length APP and N-terminal-truncated APP (SPA4CT) constructs showed similar levels of reduction in Aβ secretion after induction of dimerization.

DISCUSSION

It has been reported that APP contains a number of domains that mediate homo- and heterodimerization, the latter interacting with APLP1 and APLP2, and in support of the functionality of these domains, small amounts of APP are recovered as dimers *in vitro* and *in vivo* (17, 18, 21, 25). To date, a number of diverse physiological roles have been attributed to this dimerization event. In addition, based primarily on artificial cysteine mutations designed to induce disulfide bond formation, it has been suggested that APP dimerization accelerates Aβ production (25). However, subsequent studies have not consistently confirmed these initial observations (23, 27). In this study we chose to use a different approach to induce APP dimerization to explore the relationship between dimerization and Aβ generation without having to introduce cysteine mutations by creating APP-FKBP chimeric proteins. The addition of the bivalent compound AP20187 led to rapid and efficient formation of APP dimers in transfected cells. Fusion of one FKBP domain resulted in ~70% dimer formation, whereas fusion of two FKBP domains resulted in dimers and multimers, with almost a complete absence of APP monomers. However, when APP dimers or multimers were formed, there was a consistent decrease in Aβ secretion that ranged from 50 to 80% depending on whether one or two FKBP domains were inserted. Therefore, we conclude that APP dimerization does not directly promote Aβ generation and in fact negatively impacts Aβ production.

Previous studies analyzing the putative role of APP dimerization all used cysteine substitutions within the Aβ domain to create artificial disulfide bonds between adjacent APP molecules. This approach leads to efficient and constitutive dimerization of APP. However, inconsistent results have been

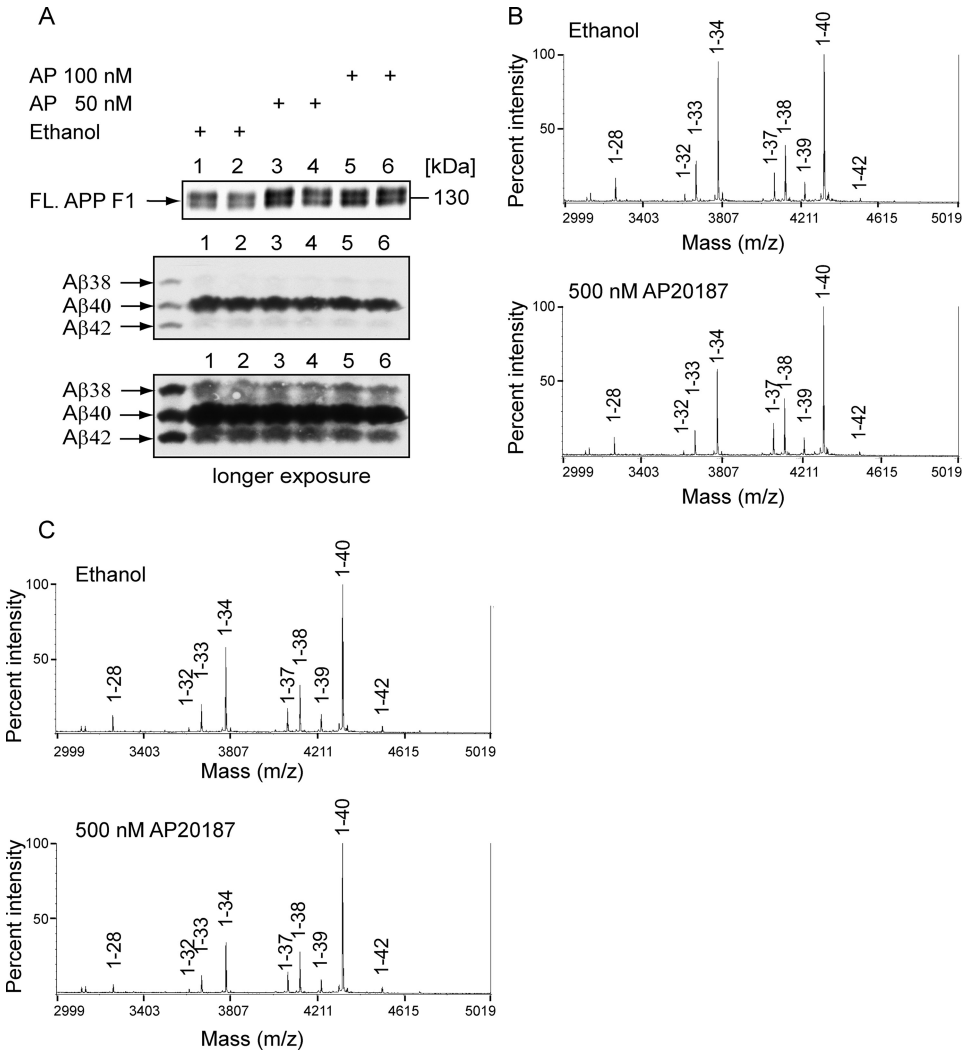

FIGURE 7. **No modulation of different Aβ species after induction of APP dimerization.** *A*, N2a cells transfected with APP695 F1 were treated overnight with 50 or 100 nM AP20187. Full-length (*FL*) APP in cell lysates was detected with an anti-HA antibody. The conditioned media were immunoprecipitated with Aβ antibody B436 and separated on a 10% Tricine-urea gel. No significant changes in the relative levels of the major Aβ species were observed. Synthetic $Aβ_{38}$, $Aβ_{40}$, and $Aβ_{42}$ peptides were run as control size markers. *B* and *C*, MALDI analysis of Aβ peptides secreted from APP695 F1 (*B*)- or APP695 F2 (*C*)-transfected N2a cells after treatment with 500 nM AP20187 as compared with ethanol treated controls.

reported regarding the effects on Aβ generation. Given the interests in the mechanisms of Aβ production, we decided to test the role of APP dimerization on APP processing by engineering APP-FKBP chimeric constructs that can be efficiently dimerized with the bivalent compound, AP20187. The advantage of this approach is that no mutations are introduced into the APP sequence, as the latter mutations may perturb processing by α-, β-, or γ-secretase by interfering with one of the enzymatic activities. For both of the published cysteine mutants (L17C and K28C), this is a critical point because, for example, the mutation L17C in APP is directly located at the α-secretase cleavage site and has the potential of interfering with α-secretase activity (21). Indeed, this is precisely the outcome we observed, as there was a significant reduction in α-secretase cleavage and a corresponding increase in β-secretase cleavage as measured by the levels of sAPPα and sAPPβ, respectively (Fig. 1). In fact, this alteration alone may explain the increase in Aβ release without potentially having to take into account any effects of actual APP dimerization. A second advantage of the FKBP-AP20187 system is the time- and concentration-dependent regulation of dimerization as compared with the constitutive dimerization of APP induced by cysteine mutations (Fig. 3). In our studies, although a tag of 122 amino acids was appended to the C terminus of APP, there were no overt perturbations in APP processing that we could observe. Both mass spectrometry and Tricine-urea gel electrophoresis showed the normal predicted profile of Aβ peptides without any alterations before or after dimerization from both APP F1 and APP F2 constructs. These findings are consistent with the apparent normal processing of APP GFP fusions used by a number of laboratories (38, 41–45). However, with this approach, our results unequivocally showed that forced dimerization of APP lowered rather than increased Aβ generation. Similar results were obtained with both full-length APP and C99 (SPA4CT) constructs, leading us to hypothesize that this reduction is due to an effect on γ-secretase cleavage and not on other aspects of APP processing, such as α- or β-secretase cleavage.

In our studies, although Aβ generation was significantly reduced, we did observe an increase in the levels of AICD after the addition of the dimerization compound. This was not expected because both Aβ and AICD are derived by γ-secretase activity (9–11), and it has been reported that the generation of Aβ and AICD are equimolar, at least under basal conditions (46). Aβ generation appears to initially start at the ϵ-cleavage near the cytoplasmic face that first releases AICD from the membrane tether, before ζ-cleavage, and finally, γ-secretase cleavages occur (47, 48). In this model these processive cleavages can be perturbed while keeping ϵ-cleavage relatively intact. In fact, a recent publication showed that mutations within the G*XXX*G motif in the APP transmembrane domain led to a reduction in Aβ40 and Aβ42 without altering AICD levels (23). In this latter case, however, the drop in Aβ40 and Aβ42 levels was accompanied by an increase in Aβ34 species (21), indicating that mutations at the G*XXX*G motif were specific for the generation of Aβ peptides, presumably due to alterations to γ-secretase cleavage. For this reason we specifically examined the profile of Aβ peptides in the APP-FKBP chimera by both Western blotting and MALDI-TOF (Fig. 7), and we did

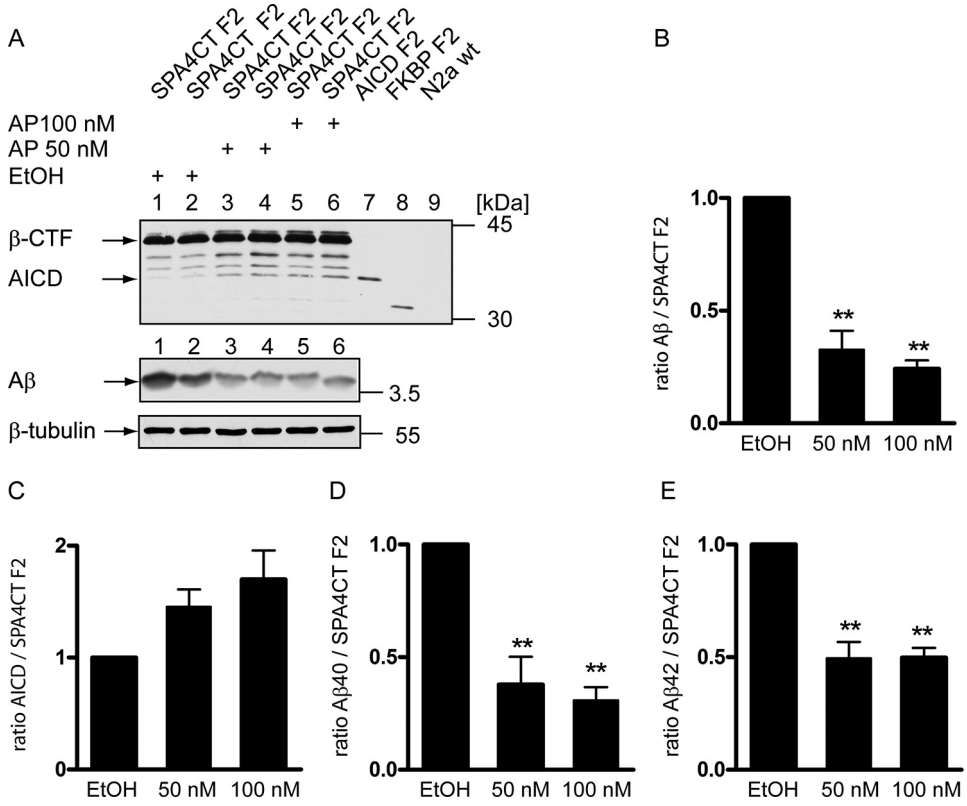

FIGURE 8. **Processing of SPA4CT F2 after induced dimerization.** *A*, N2a cells were transiently transfected with SPA4CT F2, and dimerization was induced with 50 and 100 nM AP20187 overnight. The *upper panel* shows immunoblotting of C99 and AICD fragments by an anti-HA antibody. The *middle panel* shows immunoprecipitation/Western blotting of Aβ from the treated cells. In the *lower panel* β-tubulin of cell lysates was immunoblotted with antibody E7 as a loading control. *B* and *C*, quantification of Aβ and AICD from the blots shown in *panel A* from three independent experiments ±S.D. *D* and *E*, conditioned media were also analyzed by an Aβ40 (*D*) or Aβ42 (*E*) ELISA from three different experiments ±S.D. (one-way analysis of variance followed by Tukey's post hoc analyses. *, $p < 0.05$; **, $p < 0.01$; ***, $p < 0.001$).

not detect any alterations in the profile of Aβ peptides generated from the APP-FKBP chimeric molecules before or after dimerization. Another possibility is that the stability of AICD fusion peptides is different from untagged molecules. Normally, AICD is rapidly turned over, but it is likely that the stability of AICD-FKBP fusion peptides is enhanced, a characteristic shown by other APP C-terminal fusion tags (9, 35, 38). Given this, it is possible that dimerized AICD-FKBP species are even more stable than monomeric AICD-FKBP peptides. Finally, there are other examples wherein Aβ and AICD production are not linked. For example, a number of mutations within the APP transmembrane region were shown to have distinct effects on the two cleavage events (23, 49, 50). And, TMP21, a member of the p24 cargo protein family, appeared to selectively inhibit APP processing at the γ-site without affecting ϵ-cleavage (51).

Our results are consistent with the report by Ren *et al.* (35) showing that the SPA4CT-GVP mutant K28S showed a 90% reduction of total Aβ production, whereas AICD levels were basically unaffected. Because both the K28A and K28C mutations also led to a marked reduction in Aβ secretion (Fig. 1), our results are in agreement with the observations that these mutations likely perturbed γ-secretase cleavage. In particular, although the K28C resulted in high levels of APP dimers, this itself was insufficient to augment Aβ generation and release. On the other hand, the Aβ reduction we saw in induced dimerization of APP-FKBP chimeras may be supra-physiologic, as the degree of APP dimerization that takes place normally in cultured cells appears to be far less than what was achieved by AP20187-induced dimerization. Furthermore, dimerization at the APP C terminus may not be equivalent to dimerization within other APP domains. However, it remains to be determined what percentage of APP is dimerized *in vivo*, as this has not been examined in detail. It has also been suggested that APP dimerization increases the susceptibility of cells to a variety of injury, including Aβ (24). Therefore, it is possible that even though APP dimerization may not directly impact Aβ production, this process may still play an important role in synaptic loss or neuronal death in Alzheimer disease. Last, these observations are all in accord with recent publications showing that γ-secretase is likely a monomeric rather than a dimeric complex, as was originally proposed (37, 52–54). Given these findings, γ-secretase is likely to function in the monomeric state and cleaves one rather than two substrate APP molecules within the complex.

Acknowledgments—We thank Prof. Dr. Todd Golde for Ab9, 13.1.1, and 2.1.3, Dr. Maria Kounnas for B436, and Prof. Dr. Konrad Beyreuther for WO2 antibodies, Dr. Stefan Lichtenthaler for SPA4CT DA pCEP4 and Dr. Peter Soba for APP695 pUAST and APP695 NT HA pCDNA3.1+ plasmids, ARIAD Pharmaceuticals for providing the homodimerization kit, and the University of California San Diego Mass Spectrometry facility (Drs. E. Komives and J. Torpey) for assistance.

REFERENCES

1. Glenner, G. G., and Wong, C. W. (1984) *Biochem. Biophys. Res. Commun.* **120,** 885–890
2. Masters, C. L., Simms, G., Weinman, N. A., Multhaup, G., McDonald, B. L., and Beyreuther, K. (1985) *Proc. Natl. Acad. Sci. U.S.A.* **82,** 4245–4249
3. Kang, J., Lemaire, H. G., Unterbeck, A., Salbaum, J. M., Masters, C. L., Grzeschik, K. H., Multhaup, G., Beyreuther, K., and Müller-Hill, B. (1987) *Nature* **325,** 733–736
4. Vassar, R., Bennett, B. D., Babu-Khan, S., Kahn, S., Mendiaz, E. A., Denis, P., Teplow, D. B., Ross, S., Amarante, P., Loeloff, R., Luo, Y., Fisher, S., Fuller, J., Edenson, S., Lile, J., Jarosinski, M. A., Biere, A. L., Curran, E., Burgess, T., Louis, J. C., Collins, F., Treanor, J., Rogers, G., and Citron, M. (1999) *Science* **286,** 735–741
5. Sinha, S., Anderson, J. P., Barbour, R., Basi, G. S., Caccavello, R., Davis, D., Doan, M., Dovey, H. F., Frigon, N., Hong, J., Jacobson-Croak, K., Jewett,

N., Keim, P., Knops, J., Lieberburg, I., Power, M., Tan, H., Tatsuno, G., Tung, J., Schenk, D., Seubert, P., Suomensaari, S. M., Wang, S., Walker, D., Zhao, J., McConlogue, L., and John, V. (1999) *Nature* **402,** 537–540
6. Yan, R., Bienkowski, M. J., Shuck, M. E., Miao, H., Tory, M. C., Pauley, A. M., Brashier, J. R., Stratman, N. C., Mathews, W. R., Buhl, A. E., Carter, D. B., Tomasselli, A. G., Parodi, L. A., Heinrikson, R. L., and Gurney, M. E. (1999) *Nature* **402,** 533–537
7. De Strooper, B. (2003) *Neuron* **38,** 9–12
8. Koo, E. H., and Kopan, R. (2004) *Nat Med.* **10,** (suppl.) 26–33
9. Weidemann, A., Eggert, S., Reinhard, F. B., Vogel, M., Paliga, K., Baier, G., Masters, C. L., Beyreuther, K., and Evin, G. (2002) *Biochemistry* **41,** 2825–2835
10. Sastre, M., Steiner, H., Fuchs, K., Capell, A., Multhaup, G., Condron, M. M., Teplow, D. B., and Haass, C. (2001) *EMBO Rep.* **2,** 835–841
11. Gu, Y., Misonou, H., Sato, T., Dohmae, N., Takio, K., and Ihara, Y. (2001) *J. Biol. Chem.* **276,** 35235–35238
12. Edbauer, D., Winkler, E., Regula, J. T., Pesold, B., Steiner, H., and Haass, C. (2003) *Nat. Cell Biol.* **5,** 486–488
13. Wolfe, M. S., Xia, W., Ostaszewski, B. L., Diehl, T. S., Kimberly, W. T., and Selkoe, D. J. (1999) *Nature* **398,** 513–517
14. Esch, F. S., Keim, P. S., Beattie, E. C., Blacher, R. W., Culwell, A. R., Oltersdorf, T., McClure, D., and Ward, P. J. (1990) *Science* **248,** 1122–1124
15. Wang, R., Meschia, J. F., Cotter, R. J., and Sisodia, S. S. (1991) *J. Biol. Chem.* **266,** 16960–16964
16. Dyrks, T., Weidemann, A., Multhaup, G., Salbaum, J. M., Lemaire, H. G., Kang, J., Müller-Hill, B., Masters, C. L., and Beyreuther, K. (1988) *EMBO J.* **7,** 949–957
17. Soba, P., Eggert, S., Wagner, K., Zentgraf, H., Siehl, K., Kreger, S., Löwer, A., Langer, A., Merdes, G., Paro, R., Masters, C. L., Müller, U., Kins, S., and Beyreuther, K. (2005) *EMBO J.* **24,** 3624–3634
18. Bai, Y., Markham, K., Chen, F., Weerasekera, R., Watts, J., Horne, P., Wakutani, Y., Bagshaw, R., Mathews, P. M., Fraser, P. E., Westaway, D., St George-Hyslop, P., and Schmitt-Ulms, G. (2008) *Mol. Cell Proteomics* **7,** 15–34
19. Wang, Y., and Ha, Y. (2004) *Mol. Cell* **15,** 343–353
20. Shaked, G. M., Kummer, M. P., Lu, D. C., Galvan, V., Bredesen, D. E., and Koo, E. H. (2006) *FASEB J.* **20,** 1254–1256
21. Munter, L. M., Voigt, P., Harmeier, A., Kaden, D., Gottschalk, K. E., Weise, C., Pipkorn, R., Schaefer, M., Langosch, D., and Multhaup, G. (2007) *EMBO J.* **26,** 1702–1712
22. Vooijs, M., Schroeter, E. H., Pan, Y., Blandford, M., and Kopan, R. (2004) *J. Biol. Chem.* **279,** 50864–50873
23. Kienlen-Campard, P., Tasiaux, B., Van Hees, J., Li, M., Huysseune, S., Sato, T., Fei, J. Z., Aimoto, S., Courtoy, P. J., Smith, S. O., Constantinescu, S. N., and Octave, J. N. (2008) *J. Biol. Chem.* **283,** 7733–7744
24. Lu, D. C., Shaked, G. M., Masliah, E., Bredesen, D. E., and Koo, E. H. (2003) *Ann. Neurol.* **54,** 781–789
25. Scheuermann, S., Hambsch, B., Hesse, L., Stumm, J., Schmidt, C., Beher, D., Bayer, T. A., Beyreuther, K., and Multhaup, G. (2001) *J. Biol. Chem.* **276,** 33923–33929
26. Walsh, D. M., Tseng, B. P., Rydel, R. E., Podlisny, M. B., and Selkoe, D. J. (2000) *Biochemistry* **39,** 10831–10839
27. Struhl, G., and Adachi, A. (2000) *Mol. Cell* **6,** 625–636
28. Lichtenthaler, S. F., Multhaup, G., Masters, C. L., and Beyreuther, K. (1999) *FEBS Lett.* **453,** 288–292
29. Vetrivel, K. S., Gong, P., Bowen, J. W., Cheng, H., Chen, Y., Carter, M., Nguyen, P. D., Placanica, L., Wieland, F. T., Li, Y. M., Kounnas, M. Z., and Thinakaran, G. (2007) *Mol. Neurodegener.* **2,** 4
30. Ida, N., Hartmann, T., Pantel, J., Schröder, J., Zerfass, R., Förstl, H., Sandbrink, R., Masters, C. L., and Beyreuther, K. (1996) *J. Biol. Chem.* **271,** 22908–22914
31. Levites, Y., Das, P., Price, R. W., Rochette, M. J., Kostura, L. A., McGowan, E. M., Murphy, M. P., and Golde, T. E. (2006) *J. Clin. Invest.* **116,** 193–201
32. Schägger, H., and von Jagow, G. (1987) *Anal. Biochem.* **166,** 368–379
33. Schägger, H., Cramer, W. A., and von Jagow, G. (1994) *Anal. Biochem.* **217,** 220–230
34. Kukar, T. L., Ladd, T. B., Bann, M. A., Fraering, P. C., Narlawar, R., Maharvi, G. M., Healy, B., Chapman, R., Welzel, A. T., Price, R. W., Moore, B., Rangachari, V., Cusack, B., Eriksen, J., Jansen-West, K., Verbeeck, C., Yager, D., Eckman, C., Ye, W., Sagi, S., Cottrell, B. A., Torpey, J., Rosenberry, T. L., Fauq, A., Wolfe, M. S., Schmidt, B., Walsh, D. M., Koo, E. H., and Golde, T. E. (2008) *Nature* **453,** 925–929
35. Ren, Z., Schenk, D., Basi, G. S., and Shapiro, I. P. (2007) *J. Biol. Chem.* **282,** 35350–35360
36. Clackson, T. (2006) *Chem. Biol. Drug Design* **67,** 440–442
37. Sato, T., Diehl, T. S., Narayanan, S., Funamoto, S., Ihara, Y., De Strooper, B., Steiner, H., Haass, C., and Wolfe, M. S. (2007) *J. Biol. Chem.* **282,** 33985–33993
38. Kaether, C., Schmitt, S., Willem, M., and Haass, C. (2006) *Traffic* **7,** 408–415
39. Yamasaki, A., Eimer, S., Okochi, M., Smialowska, A., Kaether, C., Baumeister, R., Haass, C., and Steiner, H. (2006) *J. Neurosci.* **26,** 3821–3828
40. Eggert, S., Paliga, K., Soba, P., Evin, G., Masters, C. L., Weidemann, A., and Beyreuther, K. (2004) *J. Biol. Chem.* **279,** 18146–18156
41. Kaether, C., Skehel, P., and Dotti, C. G. (2000) *Mol. Biol. Cell* **11,** 1213–1224
42. Rebelo, S., Vieira, S. I., Esselmann, H., Wiltfang, J., da Cruz e Silva, E. F., and da Cruz e Silva, O. A. (2007) *J. Mol. Neurosci.* **32,** 1–8
43. Chan, S. L., Kim, W. S., Kwok, J. B., Hill, A. F., Cappai, R., Rye, K. A., and Garner, B. (2008) *J. Neurochem.* **106,** 793–804
44. Florean, C., Zampese, E., Zanese, M., Brunello, L., Ichas, F., De Giorgi, F., and Pizzo, P. (2008) *Biochim. Biophys. Acta* **1783,** 1551–1560
45. Goldsbury, C., Thies, E., Konzack, S., and Mandelkow, E. M. (2007) *J. Neurosci.* **27,** 3357–3363
46. Kakuda, N., Funamoto, S., Yagishita, S., Takami, M., Osawa, S., Dohmae, N., and Ihara, Y. (2006) *J. Biol. Chem.* **281,** 14776–14786
47. Zhao, G., Cui, M. Z., Mao, G., Dong, Y., Tan, J., Sun, L., and Xu, X. (2005) *J. Biol. Chem.* **280,** 37689–37697
48. Qi-Takahara, Y., Morishima-Kawashima, M., Tanimura, Y., Dolios, G., Hirotani, N., Horikoshi, Y., Kametani, F., Maeda, M., Saido, T. C., Wang, R., and Ihara, Y. (2005) *J. Neurosci.* **25,** 436–445
49. Hecimovic, S., Wang, J., Dolios, G., Martinez, M., Wang, R., and Goate, A. M. (2004) *Neurobiol. Dis.* **17,** 205–218
50. Tesco, G., Ginestroni, A., Hiltunen, M., Kim, M., Dolios, G., Hyman, B. T., Wang, R., Berezovska, O., and Tanzi, R. E. (2005) *J. Neurochem.* **95,** 446–456
51. Chen, F., Hasegawa, H., Schmitt-Ulms, G., Kawarai, T., Bohm, C., Katayama, T., Gu, Y., Sanjo, N., Glista, M., Rogaeva, E., Wakutani, Y., Pardossi-Piquard, R., Ruan, X., Tandon, A., Checler, F., Marambaud, P., Hansen, K., Westaway, D., St George-Hyslop, P., and Fraser, P. (2006) *Nature* **440,** 1208–1212
52. Steiner, H., Winkler, E., and Haass, C. (2008) *J. Biol. Chem.* **283,** 34677–34686
53. Evin, G., Canterford, L. D., Hoke, D. E., Sharples, R. A., Culvenor, J. G., and Masters, C. L. (2005) *Biochemistry* **44,** 4332–4341
54. Schroeter, E. H., Ilagan, M. X., Brunkan, A. L., Hecimovic, S., Li, Y. M., Xu, M., Lewis, H. D., Saxena, M. T., De Strooper, B., Coonrod, A., Tomita, T., Iwatsubo, T., Moore, C. L., Goate, A., Wolfe, M. S., Shearman, M., and Kopan, R. (2003) *Proc. Natl. Acad. Sci. U.S.A.* **100,** 13075–13080